Aerofoil tones produced by a plate with cavity: the effect of acoustic forcing

Karn L. Schumacher (1), Con J. Doolan (1), and Richard M. Kelso (1)

(1) School of Mechanical Engineering, The University of Adelaide, Adelaide, Australia

ABSTRACT

A streamlined flat plate (herein 'aerofoil') containing a small rectangular cavity on one side was experimentally found to produce aerofoil tones (rather than cavity tones) under certain flow conditions. To clarify the responsible mechanism, the effect of sinusoidal acoustic forcing on the boundary layer was investigated by placing a loudspeaker downstream of the aerofoil. Velocity fluctuations in the boundary layer were then measured using a hot-wire probe. It was found that the boundary layer downstream of the cavity trailing edge responded strongly at the natural aerofoil tonal frequencies. This is due to enhanced feedback – as the naturally-occurring feedback loop is not saturated. However the shear layer over the cavity does not respond to the aerofoil's tonal frequencies. The findings suggest that an aeroacoustic feedback loop exists between the aerofoil trailing edge and cavity trailing edge.

INTRODUCTION

Generally a tone, or typically a series of tones, may be produced by the laminar or laminar-transitional flow over aerofoils. Although this phenomenon has been studied extensively, the existence of the aeroacoustic feedback loop that is considered to explain them has not yet been proven experimentally. In this study, a streamlined flat plate profile containing a small rectangular cavity on the pressure side was experimentally found to produce aerofoil tones rather than cavity tones under certain flow conditions.

The first major comprehensive study on the topic of aerofoil tonal noise was published by Paterson et al. (1973). They found that the noise consisted of a broadband contribution with central frequency, f_s, and discrete tones with frequencies, f_n. The latter were attributed to an aeroacoustic feedback loop between the noise source and laminar-transitional boundary layer over the aerofoil by various authors, most prominently by Arbey and Bataille (1983).

The details of the aeroacoustic feedback loop as reported by Arbey and Bataille (1983) are: (1) the initiation of boundary layer instabilities at some receptive point on the pressure side boundary layer, (2) the generation of acoustic waves as these instabilities pass the aerofoil trailing edge, and (3) the acoustic waves traveling upstream to the receptive point to initiate further instabilities. The result of the loop is that strong tones can be generated at the frequencies which both: (1) have the 'correct' total phase around the feedback loop, and (2) correspond to the most receptive frequencies in the region of instability of the boundary layer.

When the present authors conducted measurements of the noise produced by an aerofoil with a cavity, it was found that the plate produced aerofoil tones over the chord-based Reynolds number range of 1.0×10^5 to 1.5×10^5 at the specified angle of attack of -0.90° (where Reynolds number, Re, is a dimensionless ratio of inertial to viscous forces given by $\mathrm{Re}=CU/\nu$ where C is chord, U is freestream velocity, and ν is the kinematic viscosity of the fluid). As the majority of studies on aerofoils with cavities have addressed the issue of cavity oscillation modes over these aerofoils (for example, Lasagna et al. 2011, and Olsman et al. 2011), therefore there is limited literature with regards to the production of tones from such aerofoils.

Although a difference in tone produced by an aerofoil with compared to without a cavity was previously reported by van Osch (2008), no mechanism or explanation was proposed. However the present authors have found evidence that the cavity plays a role in the aeroacoustic feedback loop about an aerofoil (Schumacher et al. 2012). The evidence supported the existence of a feedback loop between the aerofoil trailing edge and the cavity trailing edge, as shown schematically in Figure 1. If the feedback loop exists then the boundary layer must respond to the acoustic waves generated by the flow. Therefore one avenue to investigate this further is to determine the response of the boundary layer when *external* acoustic forcing is applied. The effect of such forcing will be investigated here by the use of a loudspeaker whilst measuring the response of the boundary layer using a hot-wire velocity probe.

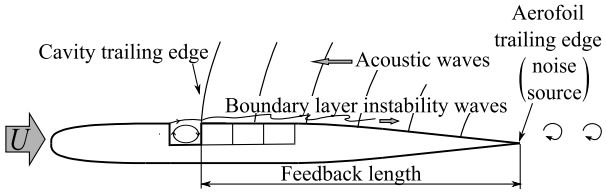

Figure 1: Simplified schematic of aerofoil tonal noise mechanism for plate with cavity.

EXPERIMENTAL METHOD

The plate with cavity profile (herein 'aerofoil') was tested in an open-jet anechoic wind tunnel facility. The dimensions of the jet are 275 mm × 75 mm. The span of the aerofoil is 275 mm, the thickness is 11 mm and the chord is 130 mm. There is a cavity which can be located in one of four positions, as shown in fig. 2(a). The dimensions of the cavity are 7 mm in chord-wise length and 6 mm in chord-normal depth.

The specification of the aerofoil consisted, from the leading edge to the trailing edge respectively, of a 33 mm long super-elliptic nose section, immediately followed a by parallel flat plate section some 35.5 mm in length (note that the nose section is immediately followed by the first cavity position on the pressure side), followed by a 61.5 mm long tail section with a 12° apex angle. An arbitrary spline curve is used in the transition between the flat plate section and the tail. The co-ordinates of the aerofoil are listed in Table 1.

The co-ordinate system used is identified in Figure 2(b). Note that the origin is always fixed at the aerofoil trailing edge, however x and y axes remain in horizontal and vertical directions, rather than chord-wise and chord-normal, regardless of

the aerofoil angle of attack.

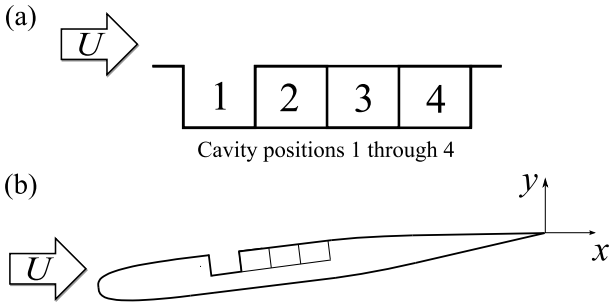

Figure 2: (a) Cavity designations, with regards to aerofoil tonal noise. (b) Co-ordinate system.

Table 1: Co-ordinates of the aerofoil, at zero angle of attack.

x/C	-1	-0.974	-0.949	-0.923	-0.885
y/C	0	0.0284	0.0341	0.0374	0.0402
x/C	-0.846	-0.788	*-0.746*	*-0.531*	-0.473
y/C	0.0416	0.0423	*0.0423*	*0.0423*	0.0423
x/C	-0.423	-0.354	-0.277	-0.154	0
y/C	0.0407	0.0364	0.0291	0.0162	0

A loudspeaker was located downstream of the aerofoil, centered at $x/C \approx 2.9$ and $y/C \approx -0.77$. The loudspeaker was facing upstream at an angle of 45° to the horizontal. At the specified angle of attack the aerofoil causes deflection of the open jet away from the loudspeaker such that there was minimal effect on the flow. The loudspeaker was driven using an amplified sinusoidal signal produced by a function generator.

The amplitude of the acoustic forcing was maintained constant for the following sets of measurements. Assuming an ideal anechoic room, the sound power level at the speaker was estimated to be approximately 88 dB re: 10^{-12} W.

The first set of measurements was taken for cavity position 1 at $U = 13.2$ m/s with geometric angle of attack, $\alpha_{\text{geom.}} = -7°$. The chord-based Reynolds number was 1.1×10^5. A hot-wire velocity probe was positioned in the pressure side boundary layer just upstream of the aerofoil trailing edge. It was positioned at a height corresponding to $u/U = 0.5 \pm 0.05$ (where u is the local velocity) and it was located at $x/C = -0.06$. The far-field noise spectrum was recorded using a B&K 0.5 in. microphone (model number 4190) positioned perpendicular to the airfoil trailing edge at $x/C = 0$ and $y/C = 4.5$. The microphone was located adjacent to the pressure side of the aerofoil. The sampling duration was 10 seconds at a sampling frequency of 50 kHz. Note that the hot-wire probe was automatically lowered into the aerofoil boundary layer using a DANTEC three-dimensional automatic traversing system, which is attached to the anechoic chamber.

The second set of measurements was taken for cavity position 1 at $U = 17.5$ m/s with $\alpha_{\text{geom.}} = -7°$. The chord-based Reynolds number was 1.5×10^5. For this set, hot-wires were positioned about the cavity. Firstly, the wire was located in the cavity shear layer downstream of the cavity leading edge ($x/C = -0.727$). Secondly, the wire was located in the boundary layer just downstream of the cavity trailing edge on the pressure surface ($x/C = -0.685$). As before, the hot-wire probe was lowered to a height corresponding to $u/U = 0.5 \pm 0.05$.

With regards to the 'true' angle of attack, since there is an open-jet the true angle of attack is less than the geometric angle of attack due to the deflection of the jet. A correction factor has been provided in the literature (Brooks et al. 1986). The corrected angle of attack is given as $-0.90°$ for $\alpha_{\text{geom.}} = -7°$. The geometric angle of attack will be quoted in the rest of the paper.

RESULTS AND DISCUSSION

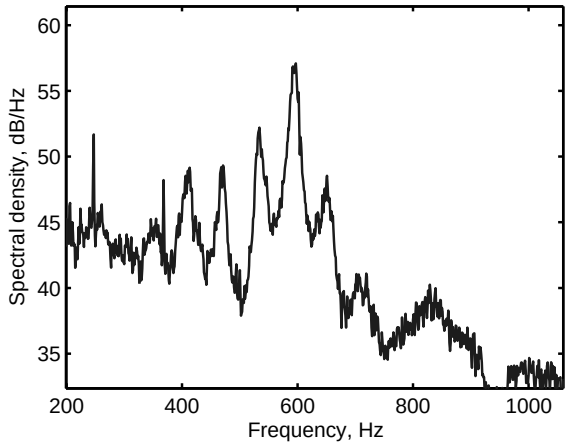

Figure 3: Far-field noise spectrum for first set of measurements. $U = 13.2$ m/s with $\alpha_{\text{geom.}} = -7°$.

Figure 3 shows the aerofoil tones present in the far-field noise spectrum, for the first set of measurements ($U = 13.2$ m/s with $\alpha_{\text{geom.}} = -7°$). As described in the literature, a series of discrete tones are found. These tones are found at approximately 413 Hz, 471 Hz, 534 Hz, 597 Hz, 651 Hz, and 719 Hz. These tones are approximately evenly spaced, at approximately 60 Hz spacing. There are also other tones at 247 Hz, 364 Hz, and 829 Hz, the latter may be the second harmonic of the tone at 413 Hz.

In addition to the approximately even frequency spacing, in Schumacher et al. (2012) it was shown that the discrete tones produced by flow over this aerofoil display a dependence on a $U^{0.85}$ power law (consistent with Arbey and Bataille (1983)) while the average behaviour of the tones follow a $f \propto U^{1.5}$ scaling relationship with freestream velocity (consistent with Paterson et al. (1973)). The tones therefore fit the behaviour expected of aerofoil tones in the literature (e.g., Kingan and Pearse (2009)).

The authors are confident that the tones are not cavity oscillation modes. Using the criterion defined by Sarohia (1977), the cavity is not expected to oscillate. The criterion is $L/\delta_0\sqrt{(\text{Re}_{\delta_0})}$ where l is the cavity length, δ_0 is the laminar boundary layer thickness at the cavity leading edge and Re_{δ_0} is the Reynolds based thereon. Note that δ_0 was estimated from the Blasius relation for a laminar boundary layer over a flat plate, from which good agreement was found with experiment in selected cases. $L/\delta_0\sqrt{\text{Re}_{\delta_0}}$ has the value 209 for this flow configuration. This is less than the required value of 290 for cavity oscillations (Sarohia 1977) – i.e., the cavity length is insufficient for cavity modes to occur at the stated chord-based Reynolds number range of the aerofoil. Furthermore, the spacing between cavity tones would be expected to be far greater than that between aerofoil tones.

The speaker was indeed able to excite hydrodynamic waves in the boundary layer for the first set of measurements. Figure

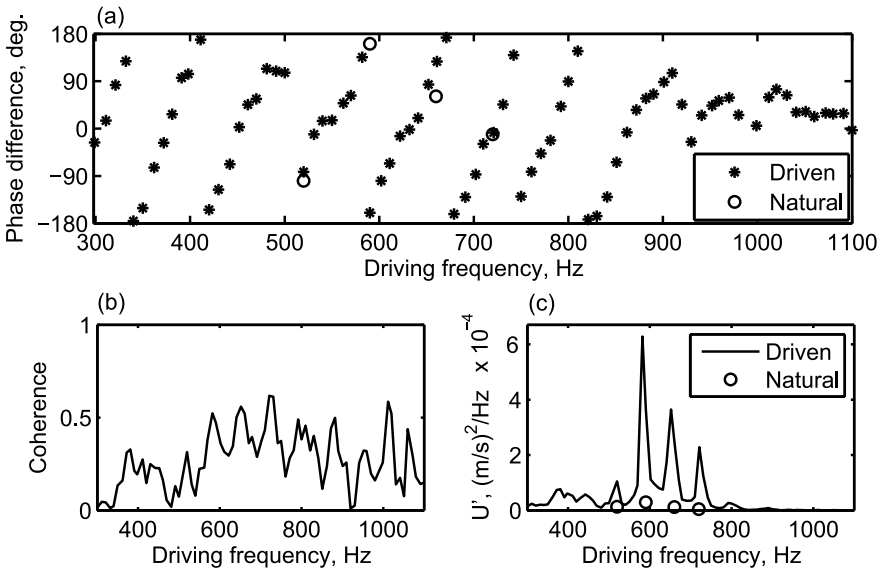

Figure 4: Properties in the pressure side boundary layer at $x/C = -0.06$ and height corresponding to $u/U = 0.5$, with acoustic forcing. (a) Phase difference (at the driving frequency) between the hot-wire and the far-field microphone. (b) Coherence (at the driving frequency) between the hot-wire and the far-field microphone. (c) Spectral density of the fluctuating velocity (at the driving frequency).

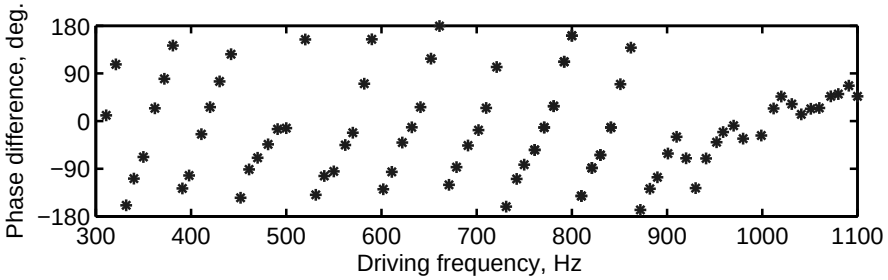

Figure 5: Properties in the pressure side boundary layer at $x/C = -0.06$ and height corresponding to $u/U = 0.5$, with acoustic forcing. Phase difference (at the driving frequency) between the hot-wire and the loudspeaker driving signal

4(a) shows the phase difference between the far-field microphone and the hot-wire. The phase difference is taken *at* the driving frequency for that particular measurement, i.e., when the driving frequency is 400 Hz then the phase difference at 400 Hz is plotted.

The phase measurement shows that convective instabilities are present at the aerofoil tonal frequencies. Hot-wires are capable of detecting the acoustic component of velocity. However, the variation in phase at the hot-wire due purely to the variation in acoustic wavelength from the speaker would be expected to be only approximately 700° or $\sim 4\pi$ radians (between 300 Hz and 700 Hz driving frequency). Clearly the actual variation in phase found is far greater than this, which shows that convective instabilities are present.

Note that the phase difference between the hot-wire signal and the loudspeaker driving signal (at the driving frequency) was also found. It can be seen in Figure 5 that the result found is similar to that obtained when the phase difference between the hot-wire signal and far-field microphone signal is taken. Therefore for the remaining sets of measurements only the latter will be plotted.

Figure 4(c) plots the spectral density of the velocity fluctuation at the driving frequency and shows that some frequencies appear to be strongly preferred compared to others. This was the case even though the acoustic forcing amplitude was maintained constant and was far greater in level than that produced naturally by the plate. The preferred frequencies are approximately spaced at 70 Hz, similar to the naturally occurring tones, and also they correspond to the naturally occurring frequencies, being located at approximately 520, 590, 660 and 720 Hz. Fig. 4(b) shows that higher coherence between the microphone and hot-wire is also found at these and other certain frequencies, also spaced at approximately 70 Hz.

The authors propose that although the speaker forces the vortices to have a certain phase, by the definition of the feedback loop at the supported frequencies, the flow-generated acoustic waves will also match in phase upstream at the coupling point. This is expected since the right number of convective wavelengths are present in order that the acoustic waves generated at the airfoil trailing edge have the required phase to travel upstream and provide reinforcement at these particular frequencies. Therefore the feedback loop still reinforces certain frequencies; the system organizes itself so that the relative phase is the same as it would be naturally, as seen in Fig. 4(a). This apparent preference for some frequencies is consistent with the existence of an acoustic feedback loop. The initial level of the convective disturbance is greater due to the forcing; therefore the flow-generated noise at the trailing edge is greater due to the stronger disturbance, and then this flow-generated noise feeds back constructively, adding to the external forcing, and so on.

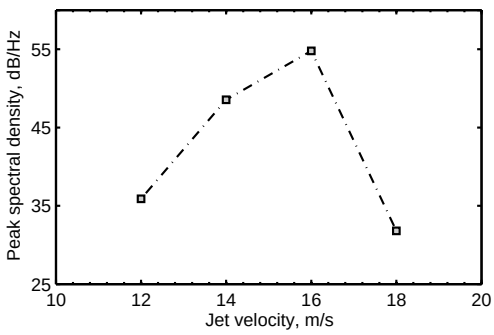

Figure 6: Peak spectral density of far-field noise versus jet velocity for a geometric angle of attack of -7°. The cavity is on the pressure side of the plate at position 1.

The spectral density of the velocity fluctuation at the peak of 582 Hz is approximately 20 times greater in the forced case than in the natural case. Presumably in the natural case, insufficient acoustic feedback is produced to saturate the mechanism. Figure 6 confirms that this particular flow configuration is below the 'plateau' in amplitude which is supposed to be indicative of a saturated feedback loop (Tam 1974). Hence there is 'room' for the boundary layer disturbances to be stronger when supplied with stronger acoustic reinforcement. However the response found is stronger at certain nearly-discrete frequencies. If there was no acoustic feedback loop, then the fluctuation strength should be proportional to the level of acoustic forcing, which was fixed, and the growth rate for the boundary layer disturbance at that frequency would be expected to vary in a smooth manner (for example, the growth rate curves given by Kingan and Pearse (2009)). That is, with no feedback loop, a smooth curve peaking at the most amplified T-S frequency would be expected, which is not the case.

To investigate the response of the aerofoil to acoustic forcing further, a second set of measurements was taken in the cavity shear layer and also just downstream of the cavity. In the cavity shear layer, only acoustic disturbances appeared to be detected at the aerofoil tonal frequencies. Figure 7 shows velocity properties in the cavity shear layer with acoustic forcing applied. The hot-wire probe was located downstream of and near to the cavity leading edge. At this position, Fig. 7(a) shows that the variation in phase found across the driving frequencies corresponds approximately to the expected variation of acoustic wavelength from the speaker suggesting that the velocity fluctuations detected at the airfoil tone frequencies are acoustic in nature. Fig. 7(c) shows that the shear layer responds to the acoustic forcing at a range of frequencies centered around 1220 Hz. The velocity fluctuation level at this frequency with the acoustic forcing applied is three orders of magnitude greater than the natural level. Figure 8 presents the natural, unforced, velocity spectrum at this location in the cavity shear layer, which shows that for the unforced case there is a broad hump present which is centered around 1230 Hz. This is likely to be a backward-facing-step vortex-shedding mode. The aerofoil tones present in this velocity spectrum are believed to be due to detection of the acoustic component of velocity only. Therefore, with forcing, the cavity shear layer appears to be responding to the acoustic forcing at the vortex shedding mode but not at the aerofoil tones. This would tend to suggest that the cavity shear layer is, expectedly, unstable (both naturally and to acoustic forcing) but only for higher frequencies than those of the airfoil tones.

Figure 9 shows the velocity spectrum for the natural unforced case, at the same location slightly downstream of the cavity trailing edge as for Figure 10. Here, a strong peak present at 560 Hz can be seen.

The point of receptivity is believed to be located near to the cavity trailing edge. Therefore the response of the boundary layer to acoustic forcing at a location slightly downstream of the cavity trailing edge is shown in Fig. 10. The phase difference here shows that convective disturbances *are* detected at the lower end of the driven frequency range, up to approximately 750 Hz. These frequencies correspond to the aerofoil tones. The spectral density of the fluctuating velocity (Fig. 10(c)) shows that the response here is strong at 560 Hz. There is a separate peak at 670 Hz. The 670 Hz peak corresponds to an aerofoil tone and the 560 Hz peak is near to the frequency of the aerofoil tone identified in far-noise spectrum for the unforced case. The spectral density of the fluctuating velocity starts to increase at the upper end of the frequency range (near the backward-facing-step frequencies) which is believed to be due to the response of the upstream cavity shear layer.

Figure 10(b) shows that the coherence is strong at the aerofoil tones. The higher coherence found upwards of 800 Hz is believed to be due to the detection of the acoustic component of velocity.

Comparing the spectral density peaks of figures 9 and 10(c), the intensity of the 560 Hz peak, when the acoustic forcing was applied, was an order of magnitude larger compared to the level found in the natural case. A second peak at 670 Hz is also present, which was three orders of magnitude larger when acoustic forcing was applied, compared to the unforced case. There are further peaks at 750 Hz and 840 Hz. The three higher frequency peaks corresponded to the aerofoil tones, which at the far-field microphone (at 1 Hz frequency resolution) were identified at 669 Hz, 753 Hz and 835 Hz.

CONCLUSION

The response of the boundary layer about an aerofoil with a cavity has been found to support the existence of an aeroacoustic feedback loop. The shear layer over the cavity reponds to acoustic forcing at backward-facing-step modes, however these frequencies are not supported by the boundary layer found downstream of the cavity and so do not contribute to the tonal noise radiated at the aerofoil trailing edge. Immediately downstream of the cavity there is a strong response to acoustic forcing at aerofoil tonal frequencies, supporting the notion that a point of receptivity in the aeroacoustic feedback loop exists near here. Closer to the aerofoil trailing edge, where amplification has occurred at the aerofoil tonal frequencies, a strong response is selectivity found at the the aerofoil tonal frequencies and the phase is found to adjust to match the phase of the naturally-occurring feedback loop. This can be explained by the external feedback enhancing the naturally occurring feedback loop – as the naturally-occurring feedback loop was not 'saturated' at this flow configuration. These findings support the aeroacoustic feedback loop model shown schematically in Fig. 1.

REFERENCES

H Arbey and J Bataille. Noise generated by airfoil profiles placed in a uniform laminar flow. *Journal of Fluid Mechanics*, 134:33–47, 1983.

T F Brooks, M A Marcolini, and D S Pope. Airfoil Trailing Edge Flow Measurements. *AIAA Journal*, 24(8):1245–1251, 1986. doi: 10.2514/3.9426.

M J Kingan and J R Pearse. Laminar boundary layer instability noise produced by an aerofoil. *Journal of Sound and Vibration*, 322:808–828, 2009. doi: 10.1016/j.jsv.2008.11.043.

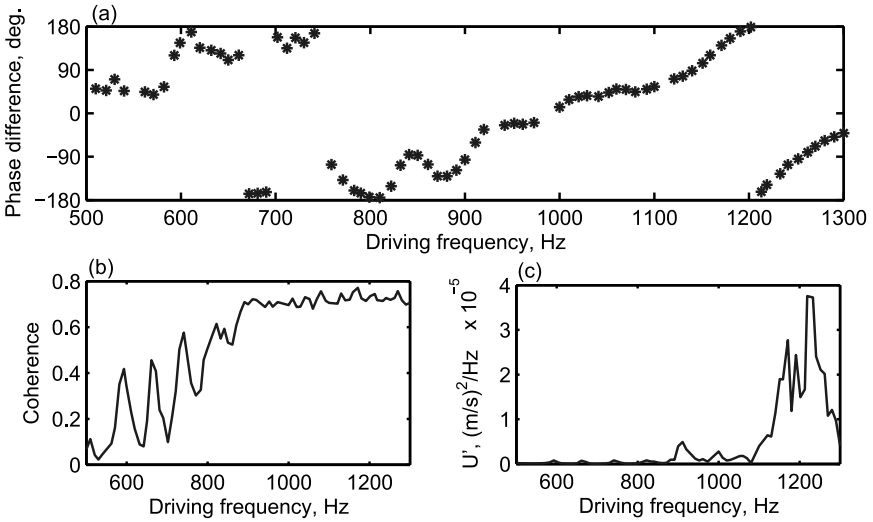

Figure 7: Velocity properties with acoustic forcing applied, with hot-wire probe at location of $x/C = -0.727$ and at height corresponding to $u/U = 0.5$ ($y/C = -0.131$). This location is in the cavity shear layer downstream of the cavity leading edge. Measurement taken at U=17.5 m/s, with cavity at position 1 and plate at -7° geometric angle of attack. (a) Phase difference (at the driving frequency) between the hot-wire and the speaker signal. (b) Coherence (at the driving frequency) between the hot-wire signal and the far-field microphone signal. (c) Spectral density of the fluctuating velocity (at the driving frequency).

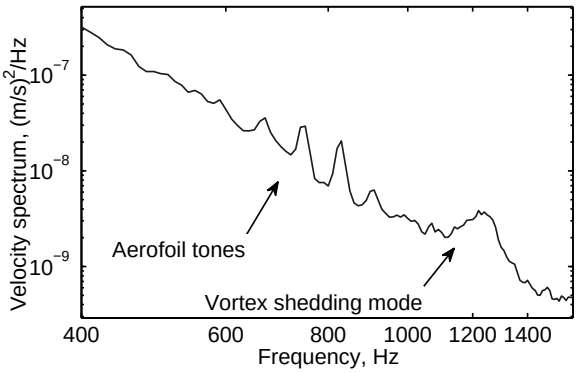

Figure 8: Velocity spectrum for the natural, unforced, case with hot-wire probe at location of $x/C = -0.727$ and at height corresponding to $u/U = 0.5$ ($y/C = -0.131$). This location is in the cavity shear layer downstream of the cavity leading edge. Measurement taken at U=17.5 m/s, with cavity at position 1 and plate at -7° geometric angle of attack.

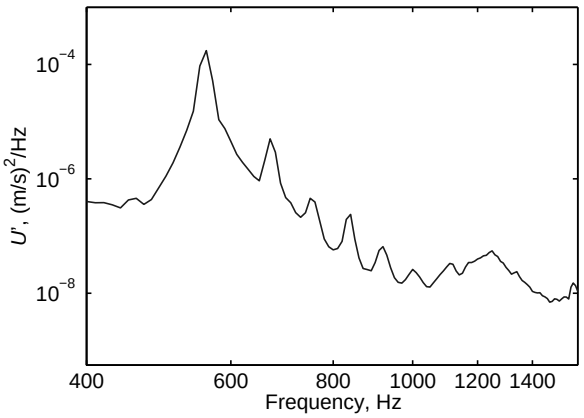

Figure 9: Velocity spectrum for the natural, unforced, case with hot-wire probe at location of $x/C = -0.685$ and at height corresponding to $u/U = 0.5$ ($y/C = -0.129$). This location is in the boundary layer, slightly downstream of the cavity trailing edge. Measurement taken at U=17.5 m/s, with cavity at position 1 and plate at -7° geometric angle of attack.

D Lasagna, R Donelli, F De Gregorio, and G Iuso. Effects of a trapped vortex cell on a thick wing airfoil. *Experiments in Fluids*, 2011. doi: 10.1007/s00348-011-1160-9.

W F J Olsman, J F H Willems, A Hirschberg, T Colonius, and R R Trieling. Flow around a NACA0018 airfoil with a cavity and its dynamical response to acoustic forcing. *Experiments in Fluids*, 51:493–509, 2011. doi: 10.1007/s00348-011-1065-7.

R W Paterson, P G Vogt, M R Fink, and C L Munch. Vortex noise of isolated airfoils. *Journal of Aircraft*, 10(5):296–302, 1973.

V Sarohia. Experimental investigation of oscillations in flows over shallow cavities. *AIAA Journal*, 15(7):984–991, 1977.

K Schumacher, C Doolan, and R Kelso. Aerofoil tones produced by a streamlined plate with cavity. In *Proceedings of 18th Australasian Fluid Mechanics Conference*, 2012.

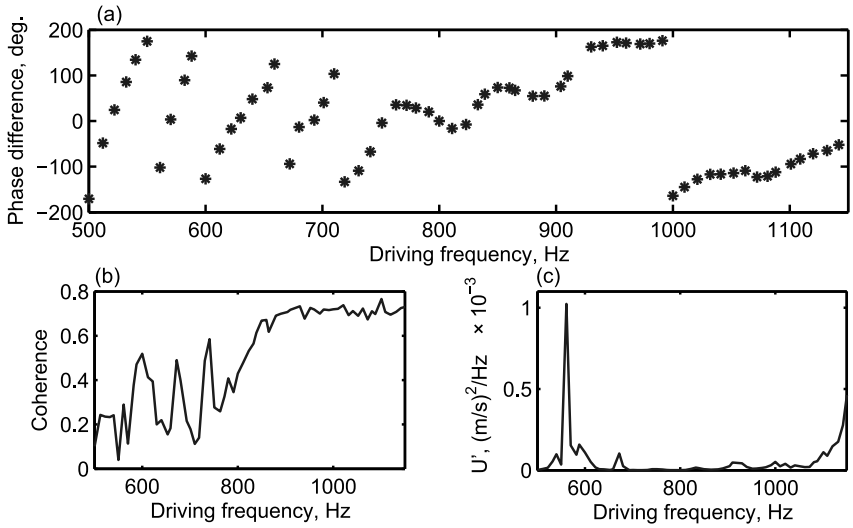

Figure 10: Velocity properties with acoustic forcing applied, with hot-wire probe at location of $x/C = -0.685$ and at height corresponding to $u/U = 0.5$ ($y/C = -0.129$). This location is in the boundary layer just downstream of the cavity trailing edge on the pressure surface of the plate. Measurement taken at U=17.5 m/s, with cavity at position 1 and plate at -7° geometric angle of attack. (a) Phase difference (at the driving frequency) between the hot-wire and the speaker signal. (b) Coherence (at the driving frequency) between the hot-wire signal and the far-field microphone signal. (c) Spectral density of the fluctuating velocity (at the driving frequency).

C K W Tam. Discrete tones of isolated airfoils. *Journal of the Acoustical Society of America*, 55(6):1173–1177, 1974.

M van Osch. Dynamics of a 2D aircraft wing with cavity: Test of a new experimental method. Master's thesis, Eindhoven University of Technology, 2008.